IEEE Transactions on Nuclear Science, Vol.NS-22, No.3, June 1975

ON THE MEASUREMENT AND INTERPRETATION OF COUPLING IMPEDANCE DATA IN THE FREQUENCY AND TIME DOMAIN

H. H. Umstatter
CERN, Geneva, Switzerland

Summary

In order to prevent beam instabilities due to the coupling impedance of vacuum tanks containing septum magnets, electrostatic inflectors, etc. in a proton synchrotron we make routine measurements with portable instruments before installation. For frequencies >20 MHz the physical size of the devices is comparable to $\lambda/4$ - the typical problem of microwave measurements - and impedance transformations by Carter- or Smith-Charts or computers are needed to obtain the true impedances. Therefore the measurement of reflection- and transmission-coefficients (S-parameters) is preferable because their magnitude is invariant along a transmission line. A center conductor of 1 cm diameter placed in our standard vacuum pipe forms a 125 Ω coaxial line. If a non-standard vacuum tank is inserted one observes reflection and transmission coefficients. To save the laborious impedance transformations in the frequency domain the reflected and transmitted waveforms are photographed in the time domain. Their interpretation in terms of frequency dependant impedances is discussed.

1. Introduction

Since the construction of the CERN proton synchrotron (CPS) in 1959 the beam intensity increased from 10^{11} to 10^{13} circulating protons due to Linac improvements and construction of the Booster synchrotron. With the increased intensity space charge effects appeared around 1965 and longitudinal instabilities[1]. They have been cured[2] by several methods like Q- or ν-jump at transition[3], "Hereward-damping"[4] of bunch shape oscillations by active feedback and Landau-damping by rf-bucket size reduction. Experience and theoretical studies led to a stability criterion for bunched beams[5]. However after acceleration the beam is adiabatically debunched for slow ejection and transfer to the future 400 GeV synchrotron (SPS). We have to obtain an order of magnitude smaller momentum spreads than the present $\Delta p/p \approx 10^{-3}$. The application of the stability criterion against self-bunching of coasting beams[6,7] poses severe limits on the acceptable coupling impedance of the old PS which has many vacuum tanks filled with electrostatic and magnetic ejection and injection equipment for beam transfer between PS and Linac, Booster synchrotron, storage rings (ISR), and experim. areas. Relatively much information on coupling impedances can be recorded with time domain reflectometers[8-10] on few photos with sweep speeds of 2,20 and 200 nsec/cm which are filed for later reference.

2. Lumped Coupling Impedance Contributions

As long as the inner vacuum chamber circumference is smaller than the wavelength λ - to preclude waveguide propagation - the coupling impedance Z_c is just the measurable impedance of the wall. The bunched beam current i_b (= charge x revolution frequency) influences equal moving surface charges on the wall which constitute a wall current i_b. This wall current is forced through Z_c and a beam-induced voltage

$$V_b = i_b \cdot Z_c \qquad (1)$$

appears. It acts on the particles like the accelerating gap voltage of an rf-cavity and perturbs them. If one increases i_b one must reduce Z_c.

a) If the wall contains short ($\ll \lambda/4$) independent sections of concentrated impedance like rf-cavities with a single gap, insulated vacuum flanges etc., a probe can be attached to it from the inside (to include all magnetic fluxes) and a lumped coupling impedance function

$$Z(s) = R + jX = |Z| \cdot e^{j\phi} \qquad (s = j\omega = j2\pi f) \qquad (2)$$

can be measured directly in rectangular or polar coordinates or with a frequency domain reflectometer. This may have an impedance overlay in rectangular (= Smith chart) or polar (= Carter chart) coordinates over its display so that it can be considered as an impedance meter with non-linear scale, capable of displaying all complex impedances with $0 \leq R \leq \infty$.

b) Sometimes gap impedances are not independent, for instance in our new rf-cavities with 2 coupled gaps or former electrostatic septum tanks in which the beam was screened over most of the tank length with gaps at two ends. These are "4 pole-networks" or "2-ports", characterized by an impedance matrix:

$$\begin{pmatrix} V_1 \\ V_2 \end{pmatrix} = \begin{pmatrix} Z_{11}(s) & Z_{12}(s) \\ Z_{21}(s) & Z_{22}(s) \end{pmatrix} \times \begin{pmatrix} i_1 \\ i_2 \end{pmatrix} \qquad (3)$$

(currents in beam direction). With the same instrument we measure directly the impedances Z_{11}, Z_{22} on gap 1 with the other gap open and Z_{1S} or Z_{2S} with the other gap short circuited. One measurement is redundant because of the reciprocity theorem for passive networks $Z_{12} = Z_{21}$. One calculates

$$Z_{12} = Z_{21} = \sqrt{(Z_{11} - Z_{1S})Z_{22}} \quad \text{or} \quad = \sqrt{(Z_{22} - Z_{2S})Z_{11}} \cdot (4)$$

For a beam with transit time τ from gap to gap currents $i_1 = i_b$, $i_2 = i_b e^{-s\tau}$ are substituted to compute V_1, V_2 and the coupling impedance:

$$Z_c = \frac{V}{i_b} + \frac{V_2}{i_b e^{-s\tau}} = Z_{11} + Z_{22} + Z_{12}\underbrace{(e^{s\tau} + e^{-s\tau})}_{2\cos\omega\tau} \qquad (5)$$

For strongly coupled gaps in symmetric tanks ($Z_{12} \approx Z_{11} = Z_{22}$) this may amount to $4Z_{11}$! 3 gaps require a 3 × 3 matrix and 6 measurements.

3. Distributed Coupling Impedances

In simple cases of uniform long pipes the length-to-circumference ratio is multiplied by the surface resistance (Ω/square, ohmmeter) and for thick metals by the skin effect surface impedance (few mΩ/sq. 1-10 MHz)

$$Z_s = \sqrt{s\mu_o\rho} = (1 + j)\sqrt{\mu_o\rho\omega/2} \qquad (6)$$

If it is not uniform we use TDR: we place a round conductor along the axis of the unknown vacuum tank to form a transmission line and terminate the far end and generator in a resistance Z_o which is the characteristic impedance which we would have with infinite standard vacuum chambers attached to both ends. In these cases the coupling impedance is defined by an integral $\int E ds$ divided by i_b, where s is in a moving frame. But even if in a large vacuum tank (circ. $\geq \lambda$) the walls have no resistance there is a coupling impedance, because the tank is a finite length of wave-guide bounded by discontinuities (→ resonator) and the electromagnetic field which goes out from the beam current is reflected and its longitudinal component acts on the beam. If the beam is simulated by a thin wire for time domain reflectometry it is seen (like distributed wall impedances in a narrow pipe) but the vacuum chamber/wire system forms a transmission line which is terminated on both ends by Z_0 and damps resonances by shunting the resonator "in the wall" by $2Z_0$ so that only impedances up to a few kΩ can be measured with reasonable precision. In high Q resonators the field can be measured better by perturbation methods, but we want to eliminate high Q-resonators anyway.

4. Relativistic Space Charge Coupling Impedance Contribution (Self fields

Even in a narrow (circ. < λ) vacuum pipe without wall resistance there is a reactive coupling impedance due to electric and magnetic "self fields" between particles. It tends to zero for relativistic particles $\beta = v/c \rightarrow 1$ and has been studied since 1959 by theorists, ref. 2) equ. 23:

$$Z_{self} = \frac{2\pi i n}{\beta c} (1/\gamma^2) \left[1 + 2\ell n\, b/a\right] \quad . \qquad (7a)$$

Here $n = \omega/\omega_{rev}$ is the harmonic number. Now we remove "theorists convention" of counting inductive reactances with negative sign ($j\omega = -i\omega$) and c.g.s.-units $4\pi/c = 377\Omega = \mu_o c$ to obtain

$$Z_{self} = -j \frac{\mu_o c\, n}{\beta\gamma^2} (\ell n\, b/a + 0.5) \quad . \qquad (7b)$$

We introduce the complex frequency s to be independent of the changing revolution frequency of protons

$$s = j\omega = jn\omega_{rev} = \frac{jn\beta c}{R} \qquad (8)$$

and find

$$Z_{self} = \frac{-sL}{(\beta\gamma)^2} = \frac{-sL}{\gamma^2 - 1} \qquad (9)$$

where

$$L = \mu_o R \left(\ell n \frac{b}{a} + 0.5\right) \qquad (10)$$

is the total accelerator inductance between the vacuum chamber of radius b and a uniformly distributed beam current within radius a. One difference between the non-conducting beam and the cylindrical center conductor in our test set-up is that on the conductor the moving charges sit on the surface ("skin effect") and therefore its distributed "ac-inductance" slightly differs from the "dc-inductance" of the beam current:

$$L' = \frac{\mu_o}{2\pi} \ell n \frac{b}{a} \quad \text{instead of} \quad L' = \frac{\mu_o}{2\pi} (\ell n\, b/a + 0.5)$$

but we could easily eliminate this difference by choosing a smaller equivalent conductor radius $r_1 = a \cdot e^{-0.5} = a \cdot 0.607$ on which the same charge produces the same transverse electromagnetic (TEM) fields but this is not necessary nor practical for standardizations because beam charge distributions are unstable. For our relativistic proton beams of 10 - 25 GeV/c ($\gamma^2 - 1 > 100$) and $b/a \approx 8$ we have per meter length

$$\frac{L'}{\gamma^2 - 1} = \frac{0.2\ \mu H/m}{\gamma^2 - 1} (\ell n\, b/a + 0.5) < 5 \cdot 10^{-3}\ \mu H/m.$$

A small correction which (in theory) one should subtract from the imaginary part of our measured complex impedances. The dc- and ac-inductance for many other geometries can be found in Grover[11] or calculated by conformal mapping onto the coaxial geometry. This yields for the standard elliptic PS vacuum chamber an equivalent radius b = 43.2 mm which is a better reference radius than the beam radius. The characteristic impedance of the coaxial system is

$$Z_o = cL' = 60\ \Omega\ \ell n\, b/r_1$$

and $L' = Z_o/c$ does not need to be calculated because its variations due to outer cross sectional changes $Z = Z_o + \Delta Z$ can be displayed with high precision versus distance x on a time domain reflectometer.

5. Differences Between Travelling Protons and TEM Waves

The purpose of our time domain reflectometer measurements is to measure differences between an ideal narrow vacuum chamber without wall resistance and reality. Secondly we have to consider the difference between a proton bunch and an electromagnetic wave both in such a perfectly conducting vacuum chamber. The TEM-waves or propagating pulse is a "photon bunch" which has no rest energy E_0 and moves with $\beta = 1$ in a very similar way as the proton bunch which moves with $\beta = \sqrt{1 - E_o^2/E^2} < 1$. Both are surrounded by similar electromagnetic fields and wall currents but for the TEM-wave the unbalance of electric and magnetic space charge forces in Z_{self} cancels because

$$Z_{self} = \frac{-sL}{\gamma^2 - 1} = sL\left(1 - \frac{1}{\beta^2}\right) \rightarrow 0.$$

So in our tests we simulate an extremely relativistic beam without special assumptions on γ and can add the small correction afterwards. Moreover the beam does not conduct (no skin effect) and when it drives a current through the high wall impedance of resonant cavities it induces very high voltages, again because it is considered as a current generator with no source conductance (= infinite source resistance) whereas our signal- or pulse-generators have a finite source conductance in parallel to an ideal current generator (e.g. $G_o = 1/50\ \Omega = 1/Z_0$) or according to Thevenins theorem in series with an equivalent voltage generator. Therefore if we drive a cavity of very low shunt conductance (= high shunt resistance) by our current pulse this cavity shunt conductance G_{cav} becomes negligible against the conductance $1/(2Z_0)$ of 2 resistive terminations and the voltage is bounded

$$V = \frac{io}{.5G_o + G_{cav}} \leq \frac{io}{.5G_o} = 2V_o \ .$$

The generator impedance must be matched to Z_o in order to absorb all reflected signals (which would otherwise be superposed to the test pulse). Thus one can increase

Z_o by choosing a thin center conductor radius

$$r_1 = b\, e^{-Z_o/60\,\Omega}.$$

So if we try to increase the source impedance to Z_o = 1 kΩ a wire of $2r_1 = 5 \cdot 10^{-3}$ mm would enormously attenuate and smooth signals. A compromise of high Z_o/ small resistance over 1 - 2 m length is r_1 = 1 or 5 mm. The latter has the advantage that for our standard vacuum chamber it yields $Z_o \simeq 125\ \Omega$ the highest standard impedance for which we find good coaxial cables and components. This is our reference. Both ends are matched in Z_o and this simulates an infinitely long standard vac. pipe into which the unknown tank is inserted. So the photon bunches are not reflected at the far end but travel one way and we have time to observe long transients which are reflected from energy storing devices like resonators or open cables connected to our straight section. These resonators are damped by $\underline{2Z_o}$ due to our 2 terminations.

6. Some Interpretation Formulas

TDR-literature[9,10] shows how to measure distributed wall impedance along transmission lines, to localize lumped obstacles and how to determine values of series or parallel R-C or L-C combinations which all 4 return exponential signals (rising for C, falling for L). We often observe damped oscillations $\rho_o e^{-t/\tau} \sin \omega t$ of which we can measure the period T, damping time constant τ and ρ_o on photos. From these 3 quantities an equivalent circuit for resonators can be derived for later use in theory:

$$\omega = 2\pi/T \qquad , \omega_o = \sqrt{\omega^2 + \tau^{-2}}$$

$$C = \frac{1}{\omega(2Z_o\rho_o)} , \quad L = \frac{1}{\omega_o^2\, C}$$

$$R = \frac{\pi\tau}{T}\, (2Z_o\rho_o) .$$

From the loaded shunt conductance $1/R$ one subtracts $1/(2Z_o)$ and finds $1/R_{sh}$ of the resonator. This subtraction limits precision. Note that $2Z_o\rho_o \simeq \sqrt{L/C}$ but not R_{sh}. In general the time derivative of $\rho(t)$ from step pulses yields the reflections from short δ-pulses. Their Laplace transform or s times the Laplace transform of $\rho(t)$ is just $\rho(s)$ in the frequency domain which yields the wall impedance $\Delta Z(s) = 2Z_o\, \rho/(1 - \rho)$.

References

1. Y. Baconnier, J. Gareyte, P. Lefèvre, 1971 Part. Accel. Conf. IEEE Trans. NS-18, p. 1027.
2. D. Boussard, J. Gareyte, D. Möhl, IEEE Trans. NS-18, p. 1073.
3. W. Hardt, G. Merle, D. Möhl, A. Sørenssen, L. Thorndahl, 7. Int. Conf. High En. Accelerators Yerevan 1969, Vol. 2, p. 329.
4. H. G. Hereward, Second order effects in beam control system of particle accelerators, 1961 Int. Conf. High En. Accelerators, p. 236.
5. F. J. Sacherer, 1973 Part. Accel. Conf. IEEE Trans. NS-20, p. 825.
6. E. Keil, W. Schnell, Concerning long. stability in the ISR, CERN-ISR-TH-RF/69-48.
7. A. M. Sessler, 1971 Part. Accel. Conf. IEEE Trans NS-18 p. 1039.
8. A. Faltens et al, 8. Int. Conf. High En. Accel., CERN 1971 p. 338.
9. B. Oliver, G. M. Cage, Electronic measurement & instrumentation, McGraw Hill 1971, p. 408.
10. A. A. Strickland et al, Time domain reflectometry measurements, Tektronix Inc. (1970).
11. F. W. Grover, Inductance calculations, D. Van Nostrand Comp. N.Y. 1946.

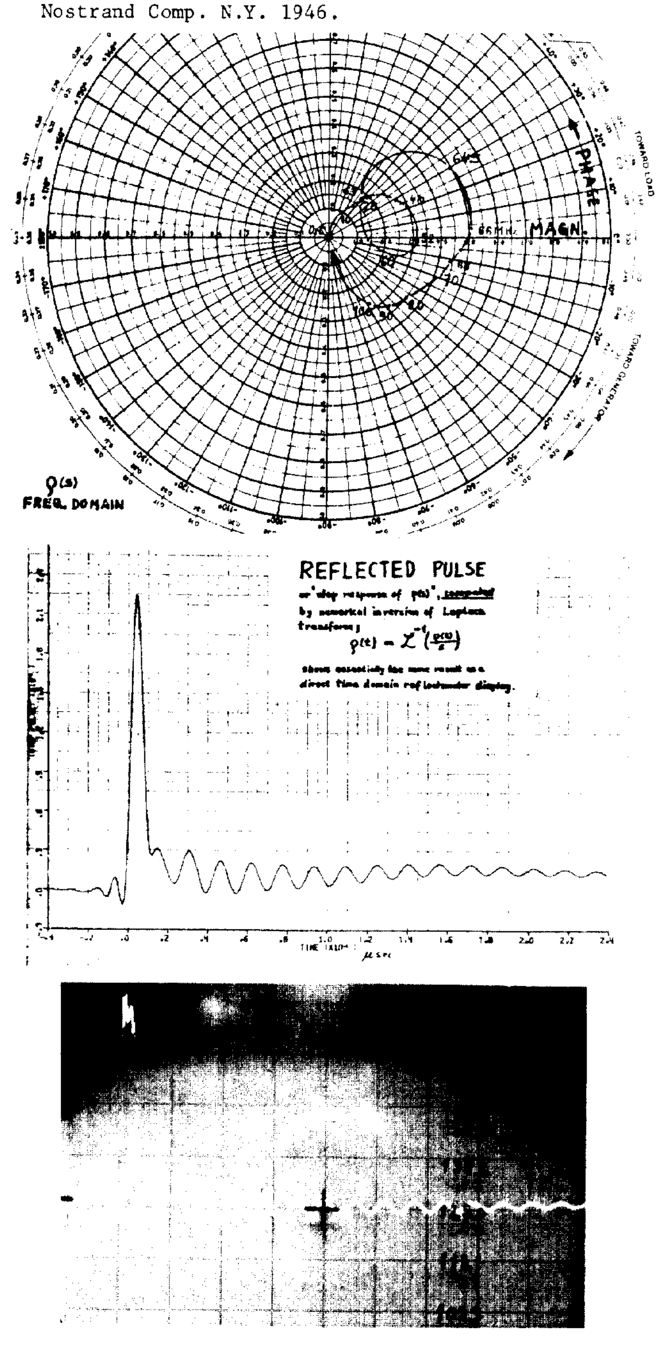

TDR-displays: ρ = 0.05/cm, 25 nsec/cm